Roberts, A. N., Berlin, V., Hager, K. M., & Yanofsky, C. (1988) *Mol. Cell. Biol. 8*, 2411–2418.
Sanger, F., Nicklen, S., & Coulson, A. R. (1977) *Proc. Natl. Acad. Sci. U.S.A. 74*, 5463–5467.
Shaw, G., & Kamen, R. (1986) *Cell 46*, 659–667.
Studier, F. W., & Moffatt, B. A. (1986) *J. Mol. Biol. 189*, 113–130.
Tsai, S. F., Martin, D. I., Zon, L. I., E'Andrea, A. D., Wong, G. G., & Orkin, W. H. (1989) *Nature 339*, 446–451.
Ullmann, A. (1984) *Gene 29*, 27–31.

Sequential ^{1}H NMR Assignments and Secondary Structure of the B Domain of Staphylococcal Protein A: Structural Changes between the Free B Domain in Solution and the Fc-Bound B Domain in Crystal†

Hidetaka Torigoe,‡,§ Ichio Shimada,‡ Akiko Saito,∥ Moriyuki Sato,∥ and Yoji Arata*,‡

Faculty of Pharmaceutical Sciences, University of Tokyo, Bunkyo-ku, Hongo, Tokyo 113, Japan, and Tokyo Research Laboratories, Kyowa Hakko Kogyo Co., Ltd., Asahimachi 3-6-6, Machida, Tokyo 194, Japan

Received April 16, 1990; Revised Manuscript Received June 6, 1990

ABSTRACT: The recombinant B domain (FB) of staphylococcal protein A, which specifically binds to the Fc portion of immunoglobulin G (IgG), has been investigated with the use of two-dimensional proton nuclear magnetic resonance spectroscopy. All backbone and side-chain proton resonances of FB (60 amino acid residues), except the amide proton resonance of Ala2, were assigned by the sequential assignment procedures by using double-quantum-filtered correlated spectroscopy (DQF-COSY), homonuclear Hartmann–Hahn spectroscopy (HOHAHA), and nuclear Overhauser enhancement spectroscopy (NOESY). On the basis of the NOESY data, three helical regions, Glu9–His19, Glu25–Asp37, and Ser42–Ala55, were identified in the free FB in solution. Existence of two of the three helical regions, Glu9–His19 and Glu25–Asp37, is consistent with the X-ray crystallographic structure of the Fc-bound FB [Deisenhofer, J. (1981) *Biochemistry 20*, 2361–2370]. By contrast, in the Fc-bound FB as revealed by the X-ray analysis, the Ser42–Glu48 segment is extended and no structural information has been available in the Ala49–Ala55 segment. We suggest that a significant conformation change is induced in the C-terminal region of FB when it is bound to the Fc portion of IgG.

Protein A is a cell wall component of *Staphylococcus aureus*. It binds specifically to the Fc portion of immunoglobulin G (IgG)[1] from various mammalian species (Langone, 1982). The primary structure was determined by the analyses of the amino acid sequence of the trypsin-digested fragment of protein A (Hjelm et al., 1975; Sjodahl, 1976, 1977a,b) and of the nucleotide sequence of the gene coding for protein A (Uhlen et al., 1984). The N-terminal part of the mature protein consists of a tandem of five highly homologous domains designated as E, D, A, B, and C, starting from the N-terminal (Sjodahl, 1977a; Uhlen et al., 1984). Each segment, which contains about 60 amino acid residues, can bind to the Fc region (Sjodahl, 1977a; Moks et al., 1986). The C-terminal part is a cell wall binding domain designated as X (Sjodahl, 1977b). This segment does not bind to the Fc region and contains approximately 180 amino acid residues (Sjodahl, 1977b).

The three-dimensional structure of the B domain (FB) bound to Fc has been solved by an X-ray crystallographic analysis of the complex between FB and the Fc fragment of human polyclonal IgG at a resolution of 2.8 Å (Deisenhofer, 1981). The electron density for the Fc-bound FB was observed for the segment from Phe6 to Glu48; no information was available for the Ala2–Lys5 and Ala49–Lys59 segments. Two antiparallel helical regions, Gln10–Leu18 and Glu26–Asp37, are the predominant elements of the secondary structure of the Fc-bound FB. The structure of FB in the free state has not been determined at the atomic level.

In the present study, we use two-dimensional proton nuclear magnetic resonance (NMR) to discuss the solution conformation of FB. A gene coding for FB was chemically synthesized, and a high-level expression system of the synthetic gene in *Escherichia coli* was established (Saito et al., 1989). The recombinant FB is a single-chain polypeptide with 60 amino acid residues (M_r 6770) containing two additional amino acids, Thr at the N-terminal and Ala at the C-terminal. Sequence-specific resonance assignments were achieved by the standard procedure (Wüthrich, 1986) and used to determine

† This research was supported in part by grants to Y.A. from the Ministry of Education, Science, and Culture of Japan (62870089 and 63430022) and from the Mitsubishi Foundation.

* To whom correspondence should be addressed.
‡ University of Tokyo.
§ Present address: Department of Physiology, Jichi Medical School, Minamikawachi-machi, Tochigi-ken 329-04, Japan.
∥ Kyowa Hakko Kogyo Co., Ltd.

[1] Abbreviations: $d_{\alpha N}(i,j)$, $d_{\beta N}(i,j)$, $d_{NN}(i,j)$, and $d_{\alpha\beta}(i,j)$, intramolecular distances between protons αCH and NH, βCH and NH, NH and NH, and αCH and βCH on residues i and j, respectively; DQF-COSY, double-quantum-filtered correlated spectroscopy; DSS, sodium 2,2-dimethyl-2-silapentane-5-sulfonate; FB, B domain of staphylococcal protein A; Fc, C-terminal half of the heavy chain of immunoglobulin; HOHAHA, homonuclear Hartmann–Hahn spectroscopy; HPLC, high-performance liquid chromatography; IgG, immunoglobulin G; NMR, nuclear magnetic resonance; NOE, nuclear Overhauser effect; NOESY, nuclear Overhauser enhancement spectroscopy; Tris-HCl, tris(hydroxymethyl)aminomethane hydrochloride.

0006-2960/90/0429-8787$02.50/0

the solution conformation of FB in the free state. The results obtained will be compared with the crystal structure of FB bound to Fc.

Materials and Methods

Expression Plasmid. A synthetic gene for FB of protein A was cloned and expressed in *E. coli* in a fused form in conjunction with a salmon growth hormone gene (Saito et al., 1989). The subcloning of the gene fragment coding for FB and salmon growth hormone, including the tryptophan promoter and the lipoprotein terminator, into a high-copy plasmid vector pTZ19R (Mead et al., 1986) produced the expression plasmid pCM1 used in the present study.

Protein Purification. E. coli MV1184 harboring pCM1 were grown in L medium (1% bactotryptone, 0.5% yeast extract, 0.5% NaCl, 0.1% glucose) containing 100 μg/mL ampicillin. FB was purified as described previously (Saito et al., 1989) with a slight modification.

The cells were harvested by centrifugation, suspended in phosphate-buffered saline (0.8% NaCl, 0.12% Na_2HPO_4, 0.02% KCl, 0.02% KH_2PO_4), and homogenized by French press. The mixture was ultracentrifuged at 29 000 rpm for 2 h. Ammonium sulfate was added to the supernatant to a concentration of 40% saturation and kept at 4 °C overnight. The precipitate collected by centrifugation was subjected to a cyanogen bromide treatment in 70% formic acid in order to cleave off the N-terminal part, which corresponds to salmon growth hormone, from the fusion protein. *N*-acetylmethionine and water were added to the reaction mixture, and the resulting mixture was centrifuged. The supernatant was applied to a Diaion SP-207 column. The fractions, which were eluted with 0.1% aqueous trifluoroacetic acid and 30% acetonitrile solution, were pooled and dialyzed against water and lyophilized. The crude protein was further purified by using an anion-exchange Mono-Q HPLC column (Pharmacia), which was eluted with a linear gradient from 0 to 200 mM NaCl, containing 20 mM Tris-HCl (pH 8.0). The main fraction was collected and dialyzed against water and lyophilized as described above. The final purification of FB was performed on a reverse-phase HPLC column (YMC Pack D-ODS-5), which was eluted with a linear gradient from 20% to 40% acetonitrile, containing 0.1% trifluoroacetic acid. The purified FB showed its homogeneity to give a single peak on a reverse-phase HPLC column. The result of the amino acid sequence determination for the three N-terminal residues was in agreement with the expected sequence. FB in this purification grade was used for the NMR analyses.

NMR Spectroscopy. NMR samples were prepared by dissolving the purified and lyophilized FB in 0.4 mL of 90% H_2O/10% D_2O at about 3.5 mM, pH 5.0, and also in 99.8% D_2O at about 3.0 mM, pH 5.0. All two-dimensional ^1H NMR experiments, DQF-COSY (Rance et al., 1983), HOHAHA (Braunschweiler & Ernst, 1983; Davis & Bax, 1985), and NOESY (Jeener et al., 1979; Macura et al., 1981), were performed on a Jeol JNM-GSX 500 spectrometer operating at 500 MHz with a probe temperature of 30 °C. Chemical shifts were measured from sodium 2,2-dimethyl-2-silapentane-5-sulfonate (DSS). DQF-COSY, HOHAHA, and NOESY spectra were recorded in the phase-sensitive mode (States et al., 1982). The water resonance was suppressed by the presaturation method. All two-dimensional spectra were recorded with 512 × 2048 data points and with a spectral width of 5000 Hz. HOHAHA and NOESY spectra were recorded with mixing times of 55 and 150 ms, respectively. Typically, 64 scans were accumulated for each t_1 with a relaxation delay of 1.2 s. A Lorentz–Gauss function for the t_2 dimension and a phase-shifted sine bell function for the t_1 dimension were applied for all two-dimensional spectra.

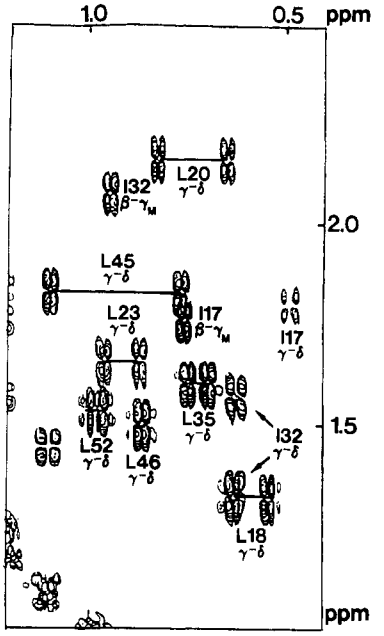

FIGURE 1: Portion of the 500-MHz phase-sensitive DQF-COSY spectrum of FB measured in 90% H_2O/10% D_2O at 30 °C, pH 5.0. The γCH–δCH$_3$ and γCH–δ'CH$_3$ cross peaks for the leucine residues and the βCH–γCH$_3$, γCH$_2$–δCH$_3$, and γ'CH$_2$–δCH$_3$ cross peaks for the isoleucine residues are labeled.

Results and Discussion

Sequence-specific resonance assignments for all backbone and side-chain protons, except the Ala2 amide proton, of FB have been carried out. Identification of amino acid spin systems was based on DQF-COSY and HOHAHA spectra and complemented with the result of NOESY measurements. The identified spin systems were ordered along the primary structure of FB through interresidue sequential NOE observed on the NOESY spectrum. The pattern of NOEs was finally interpreted in higher order structural terms for FB.

Spin System Identification. Spin systems of FB were identified primarily by using DQF-COSY and HOHAHA spectra. Direct scalar connectivities were found by the DQF-COSY spectrum, and both direct and relayed through-bond connectivities were detected by the HOHAHA spectrum (Wüthrich, 1986).

Well-resolved cross peaks in the methyl region of the DQF-COSY spectrum (Figure 1) were used for the identification of the spin systems of Leu and Ile residues. FB does not contain Val. Figure 1 shows the γCH–δCH$_3$ cross peaks for Leu and the γCH$_2$–δCH$_3$ and βCH–γCH$_3$ cross peaks for Ile. The degeneracy of the pair of δCH$_3$ resonances of Leu46 and Leu52 resulted in only one γCH–δCH$_3$ cross peak. On the basis of the analyses shown in Figure 1, the relayed connectivities of Leu and Ile were established by using the cross peak region between αCH and side-chain proton resonances of the HOHAHA spectrum (Figure 2). The spin systems for Ala and Thr residues were assigned by the magnetization transfer from αCH to βCH$_3$ for Ala and that from αCH through βCH to γCH$_3$ for Thr in the cross peak region between αCH and side-chain proton resonances of the HOHAHA spectrum (Figure 2). The αCH–βCH$_2$ cross peaks for Ser residues were obtained near the diagonal at about 4 ppm in the DQF-COSY spectrum. In the same region, no direct αCH–α'CH cross peaks of the single Gly residue could be observed, because the αCH and α'CH resonances had almost

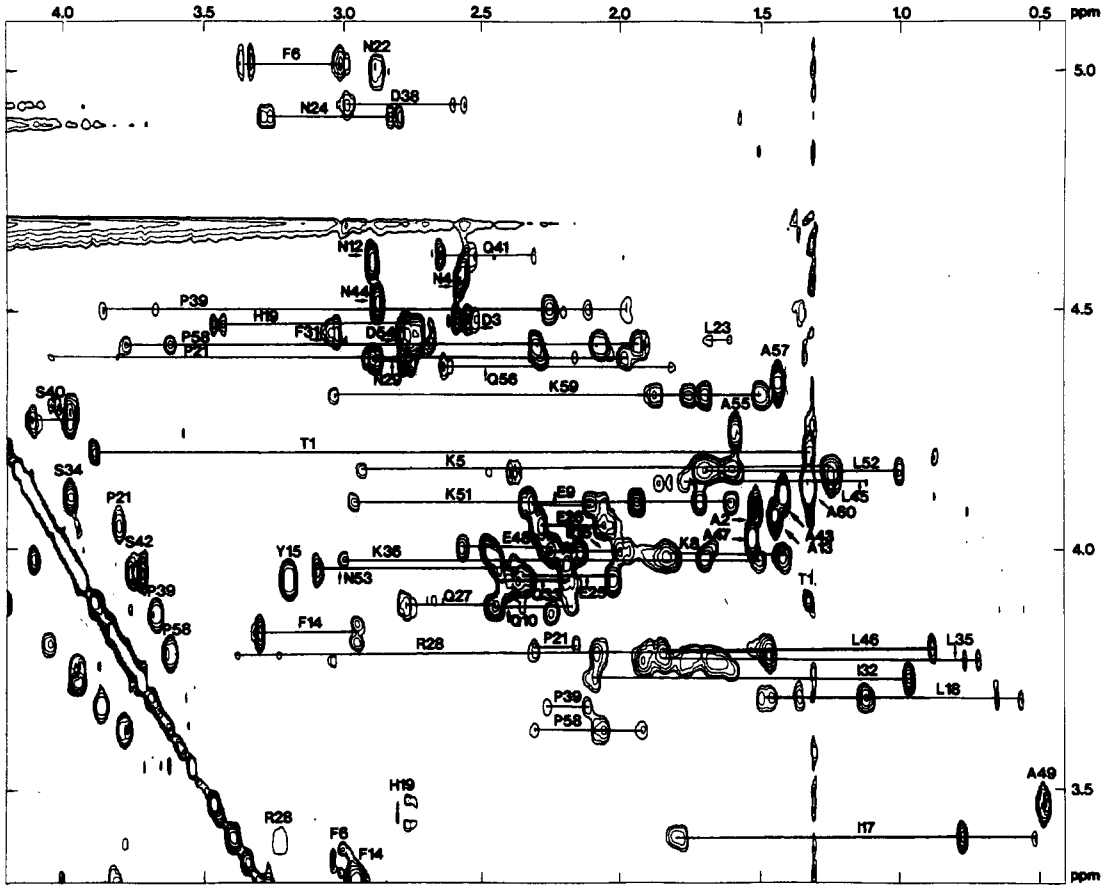

FIGURE 2: αCH aliphatic region of the 500-MHz phase-sensitive HOHAHA spectrum of FB measured in 90% H_2O/10% D_2O at 30 °C, pH 5.0. The mixing time used was 55 ms. Spin systems are connected by vertical lines and labeled.

identical chemical shifts. The Gly residue was identified by the cross peak in the αCH–NH fingerprint region on the basis of the sequential assignment described below.

Ring proton resonances of Phe, Tyr, and His residues were assigned in the aromatic region of the DQF-COSY and HOHAHA spectra. FB does not contain Trp. The assigned δCH ring protons of each amino acid residue were connected to the βCH_2 and αCH resonances by the strong NOE cross peaks in the NOESY spectrum. The βCH_2 proton resonances for these amino acids were confirmed in the αCH aliphatic region of the DQF-COSY spectrum.

The αCH–βCH_2 spin systems for Asn and Asp residues and the αCH–βCH_2–γCH_2 spin systems for Gln and Glu residues were obtained from the αCH aliphatic region of the DQF-COSY and HOHAHA spectra (Figure 2). The βCH_2 proton resonances of Asn and the γCH_2 proton resonances of Gln were identified on the basis of the NOE cross peaks between δNH_2 and βCH_2 for Asn and between ϵNH_2 and γCH_2 for Gln in the NOESY spectrum recorded in 90% H_2O/10% D_2O. Inspection of these NOE cross peaks resulted in the distinction between (Asn, Gln) and (Asp, Glu) residues.

Resonance connectivities of Lys, Arg, and Pro residues were identified in the αCH aliphatic region of the HOHAHA spectrum (Figure 2). Assignments of these amino acid types in the HOHAHA spectrum were established by matching the spin systems developed from the αCH resonance and from the ϵCH_2 resonances for Lys, and also be the coincidence of the spin systems relayed from the αCH resonance and from the δCH_2 resonances for Arg and Pro.

The assigned αCH and side-chain resonances of the various spin systems as described above were confirmed and connected to the NH resonances in the NH aliphatic region of the HOHAHA spectrum recorded in 90% H_2O/10% D_2O. All but Ala2 amide proton resonances could be observed in this region. This region of the HOHAHA spectrum also served to identify the side-chain amide protons of Arg28 and Lys59 residues.

Sequential Assignments. The sequence-specific resonance assignments can be achieved with the NOESY spectrum by standard procedures (Wüthrich, 1986). The assignments were based on the interresidue sequential NOE connectivities, $d_{\alpha N}(i,i+1)$, $d_{\beta N}(i,i+1)$, and $d_{NN}(i,i+1)$. These results were obtained by the NOESY spectrum recorded in 90% H_2O/10% D_2O with a mixing time of 150 ms.

Figure 3 shows the αCH–NH fingerprint region of the NOESY spectrum containing sequential $d_{\alpha N}(i,i+1)$ connectivities. By comparison with the same region of the DQF-COSY and HOHAHA spectra recorded in 90% H_2O/10% D_2O, it was possible to distinguish between interresidue and intraresidue NOE cross peaks observed in the NOESY spectrum. On the basis of the $d_{\alpha N}(i,i+1)$ NOE connectivities, the sequential assignments were achieved. Almost all of the expected $d_{\alpha N}(i,i+1)$ NOE connectivities were observed. The starting point of the sequential assignment shown in Figure 3 was Ser40. According to the $d_{\alpha N}(i,i+1)$ NOE cross peaks, the sequence-specific resonance assignments from Ser40 to Ala57 were accomplished. Using the identical procedure, we traced $d_{\alpha N}(i,i+1)$ NOE connectivities from Asp3 to His19, and from Asn22 to Asp38 with the exception of Asn7/Lys8 and Tyr15/Glu16. The sequence-specific assignments in these regions were also achieved.

Figure 4 indicates the NH–NH region of the NOESY spectrum containing sequential $d_{NN}(i,i+1)$ connectivities. The sequential assignments obtained from the $d_{\alpha N}(i,i+1)$ NOE connectivities were confirmed and complemented on the basis of the identification of $d_{NN}(i,i+1)$ NOE connectivities. The

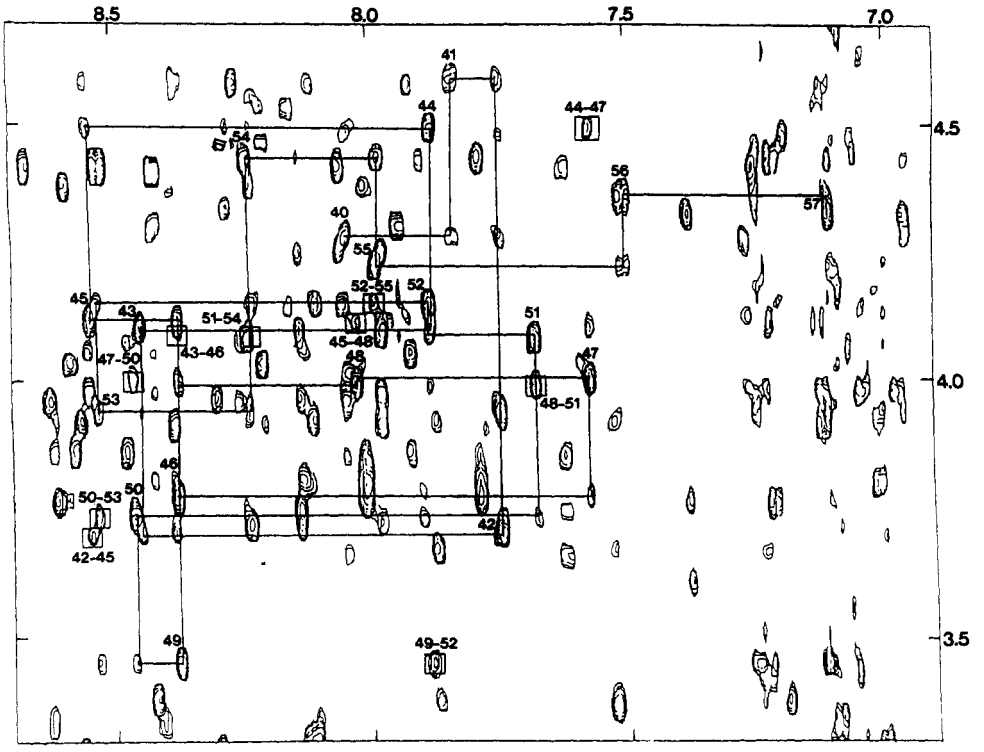

FIGURE 3: NH–αCH region of the 500-MHz phase-sensitive NOESY spectrum of FB measured in 90% H_2O/10% D_2O at 30 °C, pH 5.0. The mixing time used was 150 ms. The αCH(i)–NH(i+1) sequential NOE connectivities for the residues Ser40–Ala57 are indicated by the continuous line. The intraresidue αCH(i)–NH(i) cross peaks are labeled. The αCH(i)–NH(i+3) NOEs for the residues Ser42–Ala55 are boxed and labeled.

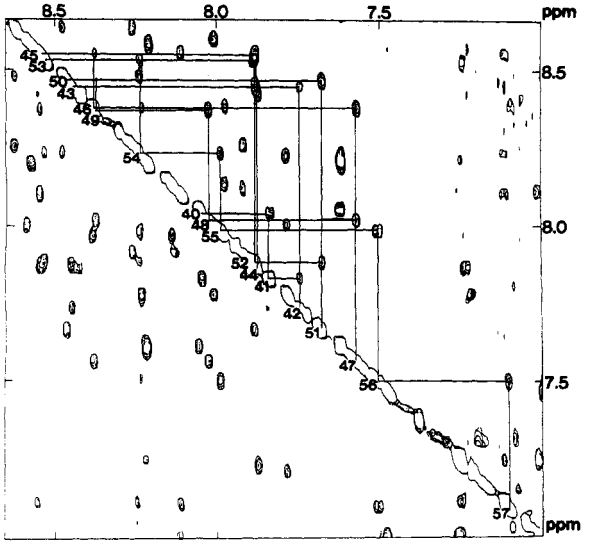

FIGURE 4: NH–NH region of the 500-MHz phase-sensitive NOESY spectrum of FB measured under the same condition as described in Figure 3. The NH(i)–NH(i+1) sequential NOE connectivities for the residues Ser40–Ala57 are indicated by the continuous lines.

$d_{NN}(i,i+1)$ NOE cross peaks were found in the same region of FB, from Ser40 to Ala57, as shown in Figure 3. In addition, we observed $d_{NN}(i,i+1)$ NOE connectivities from Glu9 to His19 and from Asn22 to Asp38 with the exception of Phe14/Tyr15, Asn24/Glu25, Gln27/Arg28/Asn29, and Lys36/Asp37. These $d_{NN}(i,i+1)$ connectivities were difficult to observe due to the overlapping NH resonances of these residues.

Sequential $d_{\beta N}(i,i+1)$ connectivities were also useful to check and complement the sequential assignment deduced from the $d_{\alpha N}(i,i+1)$ and $d_{NN}(i,i+1)$ connectivities. For Asn7/Lys8, the $d_{\beta N}(i,i+1)$ connectivity was identified, but the $d_{\alpha N}(i,i+1)$ connectivity was lost due to the coincidence of Asn7 αCH resonance with the solvent signal at 30 °C, and the $d_{NN}(i,i+1)$ connectivity could not be observed. The $d_{\alpha N}(i,i+1)$ connectivity between Tyr15 and Glu16 was missing, but $d_{\beta N}(i,i+1)$ and $d_{NN}(i,i+1)$ connectivities were detected.

Sequence-specific resonance assignments of the NH-nonbearing proline residues were achieved with the NOE connectivities between αCH(i) and $\delta CH^{Pro}(i+1)$. Actually, in the NOESY spectrum these NOE cross peaks were observed for all the Pro residues. The presence of these NOE cross peaks indicates that the $X(i-1)$–Pro(i) peptide bond takes the trans form. These assignments of the proline residues were confirmed by the $d_{\alpha N}(i,i+1)$ connectivities for Pro21/Asn22, Pro39/Ser40, and Pro58/Lys59. The complete sequence-specific resonance assignments of FB are summarized in Table I.

Secondary Structure. The $d_{\alpha N}(i,i+3)$ and $d_{\alpha\beta}(i,i+3)$ NOE connectivities in the region Ser40–Ala57 are boxed in Figures 3 and 5, respectively. The overlapping continuous medium-range NOE connectivities were detected in the region Ser42–Ala55. As already shown in Figure 4, the continuous $d_{NN}(i,i+1)$ connectivities were observed in the same region. The interresidue NOEs show the existence of α-helix in the region Ser42–Ala55. In addition, the continuous $d_{\alpha N}(i,i+3)$ and $d_{\alpha\beta}(i,i+3)$ NOE connectivities observed in the regions Glu9–His19 and Glu25–Asp37 indicate the presence of α-helices in these segments of FB. The interresidue NOE connectivities, $d_{\alpha N}(i,i+1)$, $d_{\beta N}(i,i+1)$, $d_{NN}(i,i+1)$, $d_{\alpha N}(i,i+3)$, and $d_{\alpha\beta}(i,i+3)$, observed for FB are summarized in Figure 6. On the basis of these NOE data, it may be concluded that FB contains three helical regions, Glu9–His19, Glu25–Asp37, and Ser42–Ala55, which will be designated from the N-terminal as helices I, II, and III, respectively. It should be noted that the three proline residues exist at positions 21, 39, and 58, flanking these helices.

Global Fold. By placing the defined secondary structure in sequence and adding key long-range NOEs, it is possible

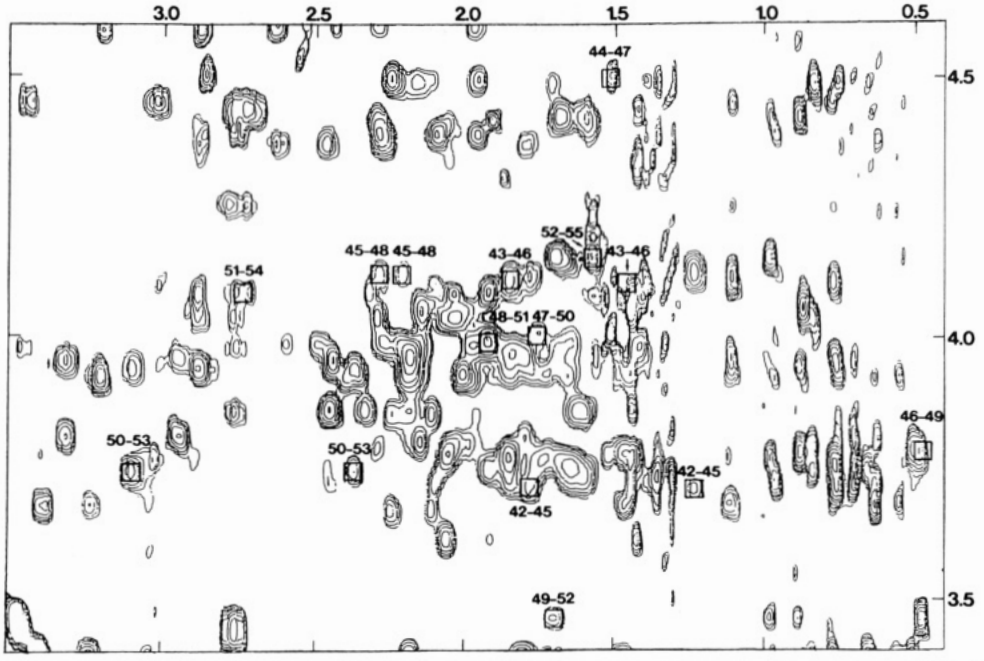

FIGURE 5: αCH aliphatic region of the 500-MHz phase-sensitive NOESY spectrum of FB measured in D_2O at 30 °C, pH 5.0. The mixing time used was 150 ms. The αCH(i)–βCH(i+3) NOEs for the Ser42–Ala55 region are boxed and labeled.

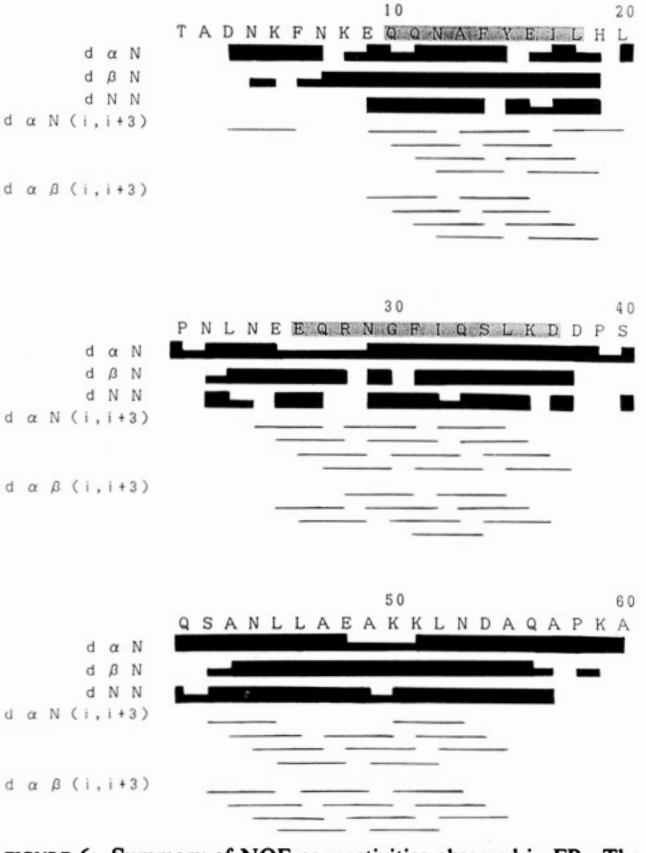

FIGURE 6: Summary of NOE connectivities observed in FB. The sequential NOEs, $d_{\alpha N}$, $d_{\beta N}$, and d_{NN}, are indicated by bars between two residues. Note that the $d_{\alpha\delta}$ connectivity for proline is included as the $d_{\alpha N}$ connectivity. The height of the bars represents the intensities of the NOEs. The medium-range NOEs, $d_{\alpha N}(i,i+3)$ and $d_{\alpha\beta}(i,i+3)$, are shown by lines between the two participating residues. The locations of the helical regions of the Fc-bound FB are indicated by shading the amino acid sequences (Deisenhofer, 1981).

to discuss a global fold of FB in solution. Existence of long-range NOEs between Phe14 δCH_2 and Leu35 δCH_3, between Ile17 δCH_3 and Phe31 βCH_2, and between Leu18 δCH_3 and Arg28 δCH_2 indicates that helices I and II are packed in an

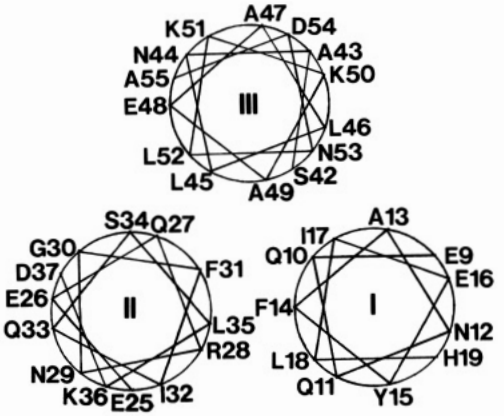

FIGURE 7: Schematic drawing of the global fold of FB. Circles indicate the three helices.

antiparallel fashion. We also conclude that helices II and III are located in an antiparallel fashion on the basis of long-range NOEs observed between Phe31 δCH_2 and Leu45 βCH_2, and between Phe31 ζCH_2 and Leu52 δCH_3. Contacts between helix I and helix III are also indicated by long-range NOEs between Ile17 NH and Leu46 δCH_3. The NOE observed between Ala57 βCH_3 and Asn22 δNH_2 shows that the C-terminal end of helix III and the loop between helix I and helix II are in spatial proximity. Existence of an NOE between Gln10 αCH and Asp38 NH indicates that the N-terminal end of helix I and the loop between helix II and helix III are also in spatial proximity. The global fold of FB deduced on the basis of these results is schematically drawn in Figure 7. It has been shown that the three helices I, II, and III have close contact to each other. Helices I and III are packed in a parallel fashion, but helix II is located in an antiparallel position with helices I and III.

Determination of the three-dimensional solution structure of FB on the basis of the NOESY data presented in this work is under way in our laboratory.

The Solution Structure of Free FB vs the Crystal Structure of Fc-Bound FB. In the present study we described the proton resonance assignments, the secondary structure, and the global

Table I: Chemical Shifts of the Proton Resonances of FB at 30 °C and pH 5.0[a]

residue	NH	αCH	βCH	γCH and others
Thr1		3.87	4.18	γCH 1.30
Ala2	ND[b]	4.06	1.50	
Asp3	8.27	4.46	2.52, 2.59	
Asn4	8.20	4.53	2.57, 2.57	δNH 6.80, 7.46
Lys5	8.15	4.14	1.61, 1.61	γCH 1.23, 1.23; δCH 1.57, 1.57; εCH 2.92, 2.92
Phe6	8.05	4.99	2.98, 3.33	δCH 7.10; εCH 7.03; ζCH 6.96
Asn7	8.39	4.70	2.92, 3.27	δNH 6.89, 7.47
Lys8	8.30	3.95	1.78, 1.83	γCH 1.40, 1.40; δCH 1.64, 1.64; εCH 2.83, 2.83
Glu9	8.24	4.07	2.03, 2.10	γCH 2.30, 2.30
Gln10	8.47	3.85	2.16, 2.16	γCH 2.42, 2.42; εNH 6.80, 7.18
Gln11	8.62	3.94	2.17, 2.17	γCH 2.42, 2.42; εNH 6.80, 7.18
Asn12	8.26	4.58	2.87, 2.87	δNH 6.96, 7.69
Ala13	7.92	4.04	1.42	
Phe14	8.13	3.80	2.92, 3.28	δCH 7.00; εCH 7.26; ζCH 7.20
Tyr15	8.10	3.91	3.18, 3.18	δCH 7.11; εCH 6.69
Glu16	8.55	3.97	1.97, 2.12	γCH 2.23, 2.23
Ile17	8.42	3.37	1.77	γCH_2 1.80, 1.80; γCH_3 0.75; δCH 0.49
Leu18	7.86	3.66	1.10, 1.45	γCH 1.33; δCH 0.54, 0.62
His19	7.23	4.44	2.74, 3.43	δCH 8.24; ζCH 7.05
Leu20	7.18	4.47	1.34, 1.70	γCH 2.17; δCH 0.65, 0.82
Pro21		4.38	1.97, 2.27	γCH 2.15, 2.15; δCH 3.78, 4.03
Asn22	8.84	4.97	2.84, 2.84	δNH 6.96, 7.38
Leu23	6.49	4.41	1.60, 1.66	γCH 1.66; δCH 0.87, 0.96
Asn24	8.52	4.88	2.79, 3.26	δNH 6.99, 7.48
Glu25	8.56	3.91	2.00, 2.00	γCH 2.32, 2.32
Glu26	8.20	4.02	2.03, 2.03	γCH 2.27, 2.27
Gln27	8.58	3.86	2.44, 2.44	γCH 2.76, 2.76
Arg28	8.61	3.76	1.46, 1.85	γCH 1.66, 1.73; δCH 3.21, 3.36; εNH 7.52
Asn29	8.59	4.38	2.75, 2.88	δNH 6.96, 7.59
Gly30	8.00	3.75, 3.75		
Phe31	7.78	4.43	3.03, 3.03	δCH 7.21; εCH 7.25; ζCH 7.11
Ile32	8.23	3.70	2.08	γCH_2 1.33, 1.57; γCH_3 0.94; δCH 0.62
Gln33	8.38	3.90	2.15, 2.15	γCH 2.39, 2.39; εNH 6.89, 7.77
Ser34	7.97	4.24	3.96, 4.09	
Leu35	8.14	3.74	1.83, 1.83	γCH 1.61; δCH 0.69, 0.74
Lys36	7.97	3.97	1.96, 1.96	γCH 1.49, 1.49; δCH 1.68, 1.68; εCH 2.98, 2.98
Asp37	8.05	4.42	2.70, 2.75	
Asp38	7.62	4.90	2.56, 2.97	
Pro39		4.48	1.94, 2.24	γCH 2.10, 2.22; δCH 3.65, 3.84
Ser40	8.04	4.28	4.02, 4.02	
Gln41	7.83	4.59	1.96, 2.61	γCH 2.28, 2.43; εNH 6.83, 7.55
Ser42	7.74	3.72	3.94, 3.94	
Ala43	8.44	4.09	1.40	
Asn44	7.88	4.49	2.86, 2.86	δNH 6.95, 7.72
Leu45	8.54	4.11	1.22, 1.76	γCH 1.83; δCH 0.76, 1.09
Leu46	8.37	3.77	1.44, 1.84	γCH 1.51; δCH 0.86, 0.86
Ala47	7.56	4.00	1.51	
Glu48	8.02	3.98	2.19, 2.27	γCH 2.46, 2.54
Ala49	8.37	3.44	0.46	
Lys50	8.46	3.73	1.74, 1.91	γCH 1.34, 1.34; δCH 1.56, 1.56; εCH 2.82, 2.91
Lys51	7.67	4.08	1.91, 1.91	γCH 1.40, 1.59; δCH 1.69, 1.69; εCH 2.95, 2.95
Leu52	7.88	4.14	1.70, 1.70	γCH 1.53; δCH 0.97, 0.98
Asn53	8.53	3.93	2.36, 3.08	δNH 6.83, 7.90
Asp54	8.24	4.43	2.70, 2.73	
Ala55	7.98	4.22	1.57	
Gln56	7.50	4.36	1.78, 2.27	γCH 2.45, 2.61; εNH 6.95, 7.27
Ala57	7.10	4.32	1.42	
Pro58		4.41	1.90, 2.29	γCH 2.05, 2.05; δCH 3.60, 3.76
Lys59	8.41	4.29	1.72, 1.84	γCH 1.48, 1.48; δCH 1.67, 1.67; εCH 3.02, 3.02; εNH 7.47
Ala60	7.94	4.11	1.30	

[a] Chemical shifts expressed in ppm relative to DSS. [b] ND, not detectable.

fold of the free FB in solution. All of the proton resonances except the amide proton resonance of Ala2 were assigned to the specific residues by the sequential assignment procedure. Secondary structure elements were identified from sequential NOEs. On the basis of several key long-range NOEs the global fold of FB was shown.

The X-ray structure of the complex between FB and an Fc fragment from human polyclonal IgG has been reported (Deisenhofer, 1981). Information available by the X-ray crystallographic study of the Fc-bound FB is limitied to the Phe6–Glu48 segment; the electron density for other parts of FB was weak and disordered. According to the X-ray data, the Fc-bound FB contains two helical regions, Gln10–Leu18 and Glu26–Asp37. The locations of the two helical regions of the Fc-bound FB are indicated by shading the amino acid sequences in Figure 6.

The existence of two helical segments, I and II, is consistent for the solution structure of the free FB determined by the two-dimensional NMR and the crystal structure of the Fc-bound FB. However, a significant structural difference exists for the C-terminal Ser42–Ala55 segment. In the free FB as seen by NMR, the Ser42–Ala55 segment forms a helical structure (helix III), whereas this portion is extended and disordered in the Fc-bound FB determined by the X-ray

crystallographic study. We conclude that a major structural change is induced in the C-terminal region of FB when it is bound to Fc. The present result is one of still relatively rare and interesting structural data, which demonstrate major structural changes between solution and crystal.

In the free FB, the three helical regions are located in close spatial proximity, interacting through the side chains of the hydrophobic residues that exist in each helix. It appears that, when FB is bound to the Fc portion of IgG through the two helices, I and II, the hydrophobic space surrounded by the three helices of FB in the free state is disrupted, resulting in a significant change in conformation of helix III comprising the C-terminal Ser42–Ala55 segment. It is also possible that the extended structure of the C-terminal Ser42–Ala55 segment has resulted from intermolecular interactions in the crystal. In order to pursue this point, a ^{15}N NMR study of the interaction between FB and IgG using uniformly ^{15}N-labeled FB is under way in our laboratory.

ACKNOWLEDGMENTS

We thank Dr. Yutaka Muto for useful discussions and Hideo Takahashi and Chigusa Matsunaga for technical assistance.

REFERENCES

Braunschweiler, L., & Ernst, R. R. (1983) *J. Magn. Reson. 53*, 521–528.
Davis, D. G., & Bax, A. (1985) *J. Am. Chem. Soc. 107*, 2820–2821.
Deisenhofer, J. (1981) *Biochemistry 20*, 2361–2370.
Hjelm, H., Sjodahl, J., & Sjoquist, J. (1975) *Eur. J. Biochem. 57*, 395–403.
Jeener, J., Meier, B. H., Bachmann, P., & Ernst, R. R. (1979) *J. Chem. Phys. 71*, 4546–4553.
Langone, J. J. (1982) *Adv. Immunol. 32*, 157–252.
Macura, S., Huang, Y., Suter, D., & Ernst, R. R. (1981) *J. Magn. Reson. 43*, 259–281.
Mead, D. A., Szczesna-Skorupa, E., & Kemper, B. (1986) *Protein Eng. 1*, 67–74.
Moks, T., Abrahmsen, L., Nilsson, B., Hellman, U., Sjoquist, J., & Uhlen, M. (1986) *Eur. J. Biochem. 156*, 637–643.
Rance, M., Sørensen, O. W., Bodenhausen, G., Wagner, G., Ernst, R. R., & Wüthrich, K. (1983) *Biochem. Biophys. Res. Commun. 117*, 479–485.
Saito, A., Honda, S., Nishi, T., Koike, M., Okazaki, K., Itoh, S., & Sato, M. (1989) *Protein Eng. 2*, 481–487.
Sjodahl, J. (1976) *FEBS Lett. 67*, 62–67.
Sjodahl, J. (1977a) *Eur. J. Biochem. 73*, 343–351.
Sjodahl, J. (1977b) *Eur. J. Biochem. 78*, 471–490.
States, D. J., Haberkorn, R. A., & Ruben, D. J. (1982) *J. Magn. Reson. 48*, 286–292.
Uhlen, M., Guss, B., Nilsson, B., Gatenbeck, S., Philipson, L., & Wüthrich, K. (1986) *NMR of Proteins and Nucleic Acids*, Wiley, New York.

Secondary Structure in Formylmethionine tRNA Influences the Site-Directed Cleavage of Ribonuclease H Using Chimeric 2′-*O*-Methyl Oligodeoxyribonucleotides†

Yoji Hayase, Hideo Inoue, and Eiko Ohtsuka*
Faculty of Pharmaceutical Sciences, Hokkaido University, Sapporo 060, Japan
Received April 3, 1990; Revised Manuscript Received May 17, 1990

ABSTRACT: In order to cleave RNA at specific positions in *Escherichia coli* formylmethionine tRNA, RNase H and complementary chimeric oligonucleotides consisting of DNA and 2′-*O*-methyl-RNA (Inoue et al. (1987) *FEBS Lett. 215*, 327] were used. Specific cleavages in the D loop, anticodon loop, TΨC loop, anticodon stem, and acceptor stem were investigated. Virtually unique hydrolyses with RNase H were observed at the TΨC loop, anticodon stem, and acceptor stem when relatively longer chimeric oligonucleotides (20-mer) were used. An efficient cleavage at the anticodon was obtained with a chimeric 13-mer when the higher structure of the tRNA was broken by hybridization with a 20-mer at the acceptor as well as the TΨC stem region. It was found that stabilities of hybrids with chimeric oligonucleotides and the presence of minor nucleosides affect the cleavage of tRNA by this approach.

Sequence-dependent cleavage of DNA by restriction endonucleases are an essential procedure for gene manipulation (Nathan & Smith, 1975). However, methods for the site-directed cleavage of RNA have yet to be developed for structural and functional studies of RNA. Although self-cleaving RNAs have been shown to act as restriction RNases (Zang et al., 1986; Haseloff & Gerluch, 1988; Koizumi et al., 1989), those RNA enzyme reactions need further investigation. RNase H, which cleaves RNA in RNA–DNA heteroduplexes (Berkower et al., 1973; Crouch & Dirksen, 1982), has been used for the sequence-dependent hydrolysis of RNA in the presence of complementary DNA. Region-specific cleavages were observed (Donis-Keller, 1979; Stepanova et al., 1979; Lorenz et al., 1987; Berger, 1987). In contrast to those experiments, chimeric oligonucleotides consisting of a tetradeoxyribonucleotide and 2′-*O*-methyl oligonucleotide serve as splints which assist unique cleavages of RNA by RNase H at the complementary site of the 5′-end of the deoxy tract (Inoue et al., 1987a). The method was shown to be applicable to the cleavage in stem regions of a transcribed RNA (Shibahara et al., 1987). Atabekov et al. (1988) have reported an experiment that involved the use of a chimeric oligodeoxyribonucleotide with an internucleotide pyrophosphate bond in the site-specific cleavage of TMV RNA. In order to cleave the formylmethionine tRNA of *Escherichia coli* at

† This work was supported in part by research grants from the Ministry of Education, Science and Culture of Japan.

0006-2960/90/0429-8793$02.50/0